Wax Layers on *Cosmos bipinnatus* Petals Contribute Unequally to Total Petal Water Resistance[1][OPEN]

Christopher Buschhaus[2], Dana Hager, and Reinhard Jetter*

Department of Botany, University of British Columbia, Vancouver, British Columbia, Canada V6T 1Z4 (C.B., D.H., R.J.); and Department of Chemistry, University of British Columbia, Vancouver, British Columbia, Canada V6T 1Z1 (R.J.)

Cuticular waxes coat all primary aboveground plant organs as a crucial adaptation to life on land. Accordingly, the properties of waxes have been studied in much detail, albeit with a strong focus on leaf and fruit waxes. Flowers have life histories and functions largely different from those of other organs, and it remains to be seen whether flower waxes have compositions and physiological properties differing from those on other organs. This work provides a detailed characterization of the petal waxes, using *Cosmos bipinnatus* as a model, and compares them with leaf and stem waxes. The abaxial petal surface is relatively flat, whereas the adaxial side consists of conical epidermis cells, rendering it approximately 3.8 times larger than the projected petal area. The petal wax was found to contain unusually high concentrations of C_{22} and C_{24} fatty acids and primary alcohols, much shorter than those in leaf and stem waxes. Detailed analyses revealed distinct differences between waxes on the adaxial and abaxial petal sides and between epicuticular and intracuticular waxes. Transpiration resistances equaled 3×10^4 and 1.5×10^4 s m^{-1} for the adaxial and abaxial surfaces, respectively. Petal surfaces of *C. bipinnatus* thus impose relatively weak water transport barriers compared with typical leaf cuticles. Approximately two-thirds of the abaxial surface water barrier was found to reside in the epicuticular wax layer of the petal and only one-third in the intracuticular wax. Altogether, the flower waxes of this species had properties greatly differing from those on vegetative organs.

The flowers of many plants are especially adapted to ensure reproductive success by attracting, orienting, and assisting pollinators. Petals must also resist unfavorable environmental conditions such as a desiccating atmosphere. Some characteristics that increase reproductive success, including their high surface areas and surface permeability to small scent molecules, may also make petals more vulnerable to drying out (Goodwin et al., 2003; Bergougnoux et al., 2007). Thus, despite their ephemeral nature, petals may need to compromise between competing physiological and ecological functions. This raises questions: How effective are petal skins at blocking water? Do petal skin compositions differ from those on other plant parts in order to balance multiple functions?

To answer these questions, both the chemical composition and the transpiration barrier properties of petal skins must be determined. It is well established that petals are covered by cuticles comparable to those on vegetative organs (Whitney et al., 2011). The waxes coating all primary parts of shoots consist of very-long-chain compounds, including alkanes, aldehydes, primary and secondary alcohols, fatty acids, esters, and ketones ranging in chain length from 20 to 70 carbons (Jetter et al., 2007). The ratio between these derivatives varies temporally and spatially between organs and layers within the cuticle (Jenks et al., 1995, 1996; Jetter and Schäffer, 2001). As well, wax may contain cyclic compounds such as pentacyclic triterpenoids (Buschhaus and Jetter, 2011). Even though it has long been known that the waxes, rather than the accompanying cutin polymer, are essential for the cuticular transpiration barrier (Schönherr, 1976), it is currently not clear how individual wax components contribute to this physiological function.

In contrast to other organs, relatively few studies so far have addressed the chemical composition of petal waxes. Noteworthy exceptions are detailed analyses of petal waxes for *Crataegus monogyna* and three cultivars of *Rubus idaeus* (Griffiths et al., 2000), *Antirrhinum majus* (Goodwin et al., 2003), *Vicia faba* (Griffiths et al., 1999), *Cistus albidus* (Hennig et al., 1988), *Petunia hybrida* (King et al., 2007), Arabidopsis (*Arabidopsis thaliana*; Shi et al., 2011), and *Rosa damascena* (Stoianova-Ivanova et al., 1971). Selected compound classes have been investigated for some more species, including selected Ericaceae (Salasoo, 1989), Rosaceae (Wollrab, 1969a, 1969b), and Asteraceae (Akihisa et al., 1998) species. Some major plant families, such as the Asteraceae, have not been investigated in much detail.

Along with chemical analyses, the physiological properties of waxes on fruits and leaves of diverse plant

[1] This work was supported by the Natural Sciences and Engineering Research Council of Canada, the Canada Foundation for Innovation, and the Canada Research Chairs Program.

[2] Present address: Crandall University, 333 Gorge Road, Moncton, New Brunswick, Canada E1C 9L7.

* Address correspondence to reinhard.jetter@botany.ubc.ca.

The author responsible for distribution of materials integral to the findings presented in this article in accordance with the policy described in the Instructions for Authors (www.plantphysiol.org) is: Reinhard Jetter (reinhard.jetter@botany.ubc.ca).

[OPEN] Articles can be viewed without a subscription.

www.plantphysiol.org/cgi/doi/10.1104/pp.114.249235

species also have been investigated in the past. The effectiveness of a water barrier may be characterized by quantifying the permeance for water (P; m s^{-1}) or, inversely, the transpiration resistance (s m^{-1}; Riederer and Schreiber, 1995). These characteristics may, in turn, be determined by measuring the water flux (J; kg m^{-2} s^{-1}) across the cuticle under controlled conditions according to the equation $P = J/\Delta c$ (where Δc is the water concentration gradient driving the diffusion across the barrier). Because both permeance and resistance are physiological characteristics independent of water concentration, their values enable comparisons between water barriers of different plant species and organs. Water permeance values and the corresponding barrier effectiveness vary widely between plant species and organs, with a range of 0.36 to 200 $\times$ 10^{-6} m s^{-1} (Kerstiens, 1996; Schreiber and Riederer, 1996). The mean and median leaf permeances (1.42 $\times$ 10^{-5} and 0.58 $\times$ 10^{-5} m s^{-1}, respectively) were lower than those of fruit (9.93 $\times$ 10^{-5} and 9.46 $\times$ 10^{-5} m s^{-1}), leading to the conclusion that leaves typically produce a better barrier against water movement than does fruit (Kerstiens, 1996). This difference in the physiological performance of waxes on different organs raises the question of how effective the transpiration barrier of cuticular waxes on petals may be. However, to date, water permeance values for petals have not been published and thus cannot be compared with those for other organs.

To fill important gaps in our understanding of cuticle function and composition, we initiated a detailed analysis of petal waxes using *Cosmos bipinnatus* as a first model. We recently reported the identification of novel compounds from the *C. bipinnatus* petal waxes (Buschhaus et al., 2013) but not the overall wax composition of the petal waxes. Therefore, the ray flowers of this species were examined here to determine (1) the wax composition on the adaxial and abaxial petal surfaces in comparison with the stem and leaf wax and (2) the corresponding petal water permeances.

RESULTS

Four sets of experiments were carried out on petal and leaf surfaces from *C. bipinnatus*: (1) the true surface areas of both petal sides were determined as references for both water permeabilities and wax coverages; (2) water permeabilities of the various wax compartments were measured, distinguishing between waxes on both sides of the petal and the epicuticular and intracuticular wax layers on the abaxial side; (3) chemical analyses were performed with increasing spatial resolution, starting with total petal waxes, then discriminating between waxes on both sides of the petal and then also between the epicuticular and intracuticular wax layers on the abaxial side; and (4) leaf and stem wax compositions as well as leaf permeabilities were analyzed for comparison.

Epidermal Cell Shapes

Scanning electron microscopy was used to investigate the microrelief of the petal surfaces and to determine their three-dimensional surface areas. Neither the adaxial nor the abaxial surface contained stomata or trichomes. However, the surface shapes of epidermal pavement cells differed between both petal sides (Fig. 1). The abaxial surface showed minor undulations in cross section (Fig. 1, A and B), and the true surface area of the microscopic relief is thus close to the macroscopic, projected area. Consequently, the abaxial surface area of the petal could be determined directly using the macroscopic outlines of the petal. In contrast, the adaxial surface was formed by papillose cells (Fig. 1, A, C, and D) that averaged 33 $\pm$ 5 μm in bottom diameter and 45 $\pm$ 8 μm in height (height difference between the cell tip and margin; n = 53 for both measurements). Assuming paraboloid shapes for the epidermis cells, the true surface area was enlarged by a factor of 3.8 $\pm$ 0.5 over the projected area. All further chemical and physiological measurements were referenced against this three-dimensional surface area. No epicuticular wax crystals were visible on either surface.

Water Permeances and Resistances

The macroscopically flat, astomatous, abaxial surface of the petals allowed water loss across its cuticle to be measured. However, the fragile nature of petals led to ruptures in approximately 25% of the samples in the initial sample handling steps, mostly during mounting and equilibration. Corresponding samples were discarded upon visual inspection prior to water loss measurements. For the remaining samples, water loss was (nearly) linear over several hours, with best-fit linear regressions of $r^2 > 0.97$ for 90% of the specimens. The other 10% of the samples had clearly lower regression coefficients and were excluded from further

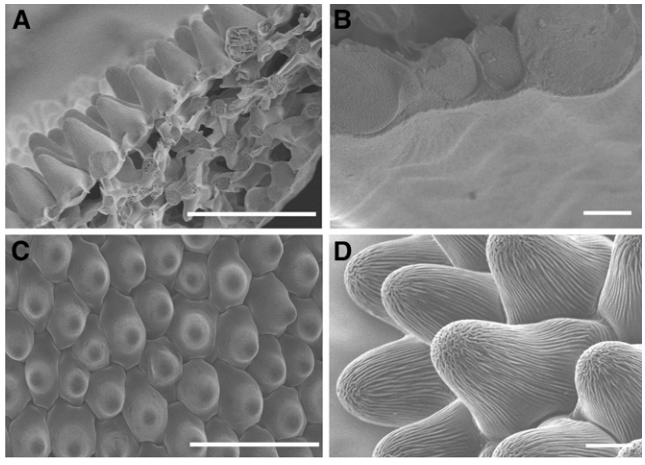

Figure 1. Scanning electron micrographs of *C. bipinnatus* petals. A, Cross section spanning the entire petal from the adaxial to the abaxial epidermis. B, Partial cross section of the abaxial epidermis and view of its surface. C, Face-on view of the adaxial surface. D, Detail of the adaxial surface. Bars = 50 μm in A and C and 10 μm in B and D.

calculations as outliers. Petal cuticles showed substantial individual variability (Fig. 2A). Taking the driving force into account, water permeances for individual cuticle samples could be calculated, and the variability of permeance values between individual specimens is illustrated in Figure 2B. Overall, the mean abaxial water permeance was $6.7 \pm 0.5 \times 10^{-5}$ m s^{-1} (n = 29). In contrast, the mean permeance for the adaxial surface was $1.3 \pm 0.1 \times 10^{-4}$ m s^{-1} (n = 26) based on the apparent macroscopic surface and $3.4 \pm 0.3 \times 10^{-5}$ m s^{-1} taking the extra surface area caused by the papillose cell shape into account (Fig. 2B).

The corresponding water resistances for the abaxial and adaxial surfaces of *C. bipinnatus* 'Sensation Pinkie' were $1.5 \pm 0.2 \times 10^4$ and $3 \pm 0.3 \times 10^4$ m s^{-1}, respectively (Fig. 3A). The total petal surface resistance calculated from these two values was similar to the experimental value obtained from whole-petal weight loss curves for the same cultivar. Independent experiments gave very similar results for the total, adaxial, and abaxial petal water resistances for a second cultivar, *C. bipinnatus* 'Sonata,' grown under different conditions (Fig. 3A).

In order to determine the contribution of the epicuticular and intracuticular wax layers to the overall barrier properties, water loss was measured after adhesive removal of the epicuticular wax layer with gum arabic and independently after extraction of the total wax (comprising both epicuticular and intracuticular waxes) with chloroform. From the resulting permeances (Fig. 3A), resistances of the individual layers were calculated, assuming that both resistances acted in series. Approximately two-thirds of the barrier function was found to reside in the epicuticular wax layer and only one-third in the intracuticular wax (Fig. 3B). Drying experiments further showed that (whole) leaf resistances were approximately 40% of corresponding (whole) petal resistances (Fig. 3A).

Total Petal Wax Composition

In order to establish the overall wax amount and composition, entire petals were dipped into chloroform using standard methods for extracting cuticular lipids. *C. bipinnatus* petals were coated with 2.7 ± 0.4 μg cm^{-2} wax. Half of the wax consisted of primary alcohols (1.5 ± 0.1 μg cm^{-2}), while the rest were alkanes (0.43 ± 0.03 μg cm^{-2}), fatty acids (0.26 ± 0.02 μg cm^{-2}), triterpenoid alcohols (0.11 ± 0.01 μg cm^{-2}), triterpenoid esters (0.08 ± 0.01 μg cm^{-2}), and traces of triterpene ketone as well as alkyl esters (both less than 0.01 μg cm^{-2}; Fig. 4). The remaining 0.36 ± 0.08 μg cm^{-2} of the gas chromatography (GC)-detected wax compounds could not be identified.

The chain length distributions and predominant compounds varied between classes (Fig. 5). Primary alcohols ranged from C_{20} to C_{30}, with mainly even numbers of carbons. C_{22} and C_{24} alcohols dominated and were also esterified to C_{16} acid in the only two esters detected. Alkane chain lengths ranged from 23 to 31 carbons, with C_{27} and C_{29} alkanes present in greatest amounts. Because C_{25} alkane could not be separated from contaminating compounds by GC, the alkanes were isolated by thin-layer chromatography (TLC) prior to GC analysis. From this, the quantity of C_{25} alkane was

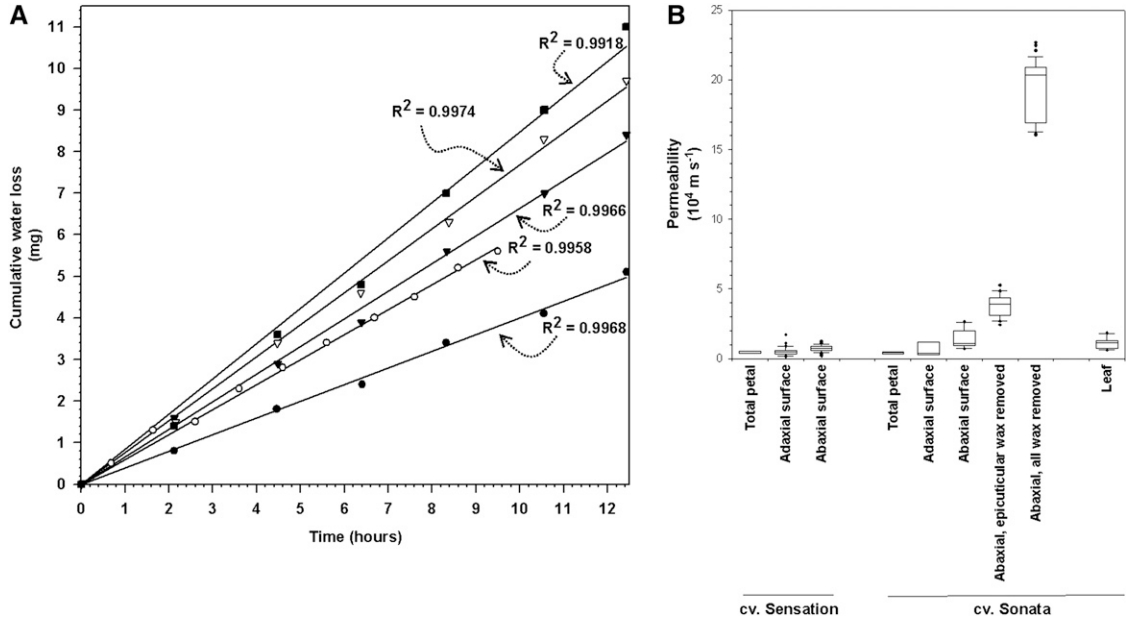

Figure 2. Analysis of cumulative water loss across individual petal cuticle samples. A, Results for five individual specimens of abaxial petal surfaces, together with best-fit linear regression lines, selected to illustrate the range of permeability values (top and bottom lines) as well as specimens near the 25%, 50%, and 75% percentiles. B, Individual variability of permeance values calculated from cumulative water loss results, showing 25%, 50%, and 75% percentiles as well as all outliers for each type of petal cuticle sample.

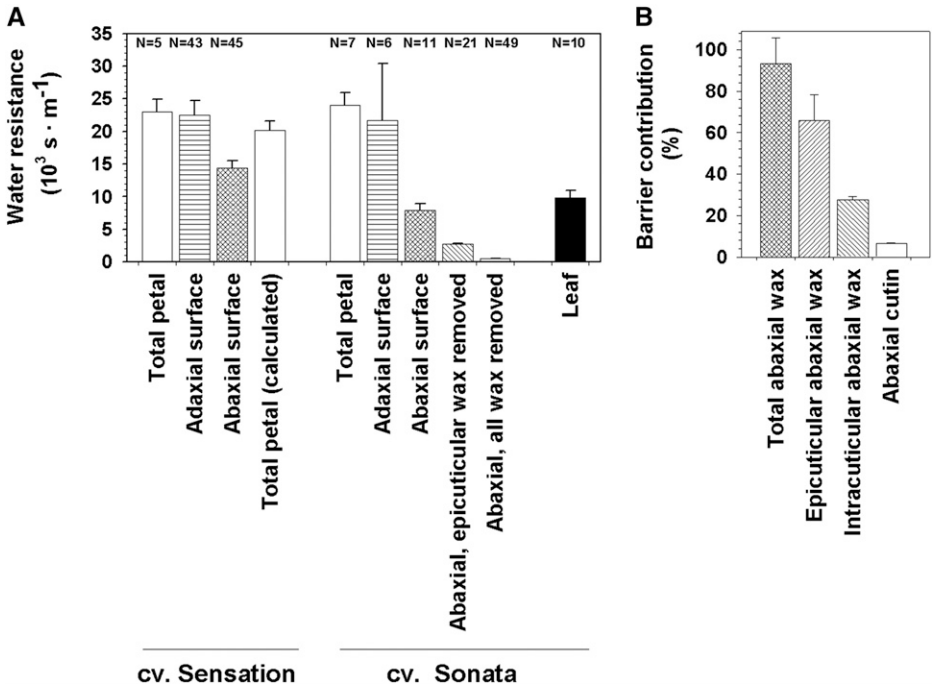

Figure 3. Water resistances and corresponding barrier contributions. A, Water resistances (10^3 s m^{-1}; geometric means ± SE) were measured for the whole petal as well as the adaxial and abaxial surfaces of *C. bipinnatus* petals 'Sensation Pinkie' and 'Sonata.' The separate values for the two sides were used to calculate the weighted average for the 'Sensation Pinkie' total petal. For the 'Sonata' abaxial petal surface, water resistances were also measured after removing only the epicuticular wax or the epicuticular and intracuticular waxes together. The water resistance of the 'Sonata' leaf surface was determined as a reference. B, From the 'Sonata' resistance values, relative contributions (%) of the total wax as well as the epicuticular and intracuticular wax layers were calculated.

calculated to be 0.05 μg cm^{-2}. Two triterpenoid alcohols, β-amyrin and α-amyrin, were found in a ratio of approximately 3:1.

Adaxial and Abaxial Petal Wax Compositions

To further investigate whether the adaxial and abaxial waxes had different compositions, both petal sides were extracted and analyzed independently (Fig. 4). The adaxial and abaxial cuticles contained 2.2 ± 0.4 and 2.8 ± 0.6 μg cm^{-2} wax, respectively. Primary alcohols constituted 70% of the adaxial wax but only 45% of the abaxial wax. Conversely, the relative abundances of abaxial alkanes (20%) and triterpenoids (10%) were twice as high as those in adaxial wax (10% and 5%). Alkyl esters were detected only in the adaxial cuticle.

The specific compounds present in the adaxial and abaxial waxes closely matched the bulk composition, but chain length distributions within classes differed between the two surfaces (Fig. 5). The C_{22} (55%) and C_{24} (35%) primary alcohols were most abundant on the adaxial surface. On the abaxial surface, they were also dominant but in reverse proportions (30% and 50%, respectively). An opposite effect was found in the alkanes, where the C_{27} and C_{29} homologs constituted 35% and 60% of the adaxial alkanes, respectively, but inversely 60% and 30% on the abaxial surface. β-Amyrin and α-amyrin occurred in ratios of approximately 4:1 and 3:1 in the abaxial and adaxial waxes, respectively.

Epicuticular and Intracuticular Abaxial Wax Compositions

Adhesive was used to mechanically sample the epicuticular wax from the abaxial side, and chloroform extraction then yielded the intracuticular wax. The epicuticular wax contained more fatty acids, primary alcohols, alkyl esters, and alkanediols than the intracuticular wax (Fig. 6). Conversely, the intracuticular wax was enriched in triterpenoid alcohols and esters. Alkanes were the only compound class found in equal concentrations in the epicuticular and intracuticular waxes. The weighted average composition

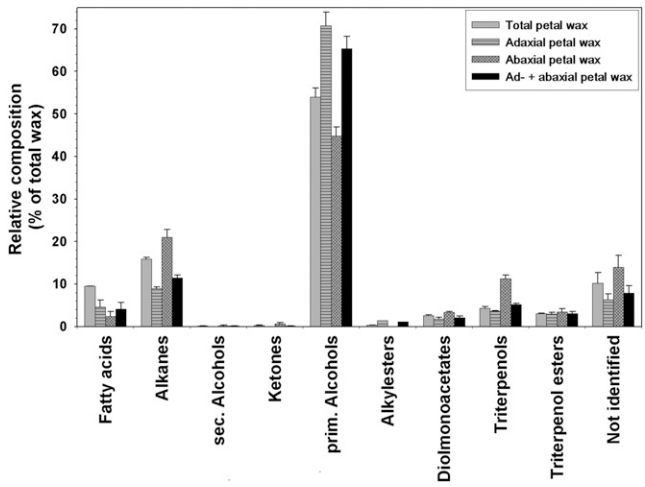

Figure 4. Relative composition of cuticular waxes on both sides of the *C. bipinnatus* 'Sensation Pinkie' petal. Relative amounts of compound classes (percentage of total wax) are shown for the wax mixtures extracted from whole petals, the adaxial or abaxial side (experimental data; gray bars), or for the combined adaxial and abaxial wax composition (calculated data; black bars). The latter was calculated as weighted averages of the adaxial and abaxial waxes to represent the total petal composition determined in two separate steps, for comparison with the experimental values determined directly (plain gray bars; averages ± SD; n = 6 for total and abaxial waxes, n = 5 for adaxial wax).

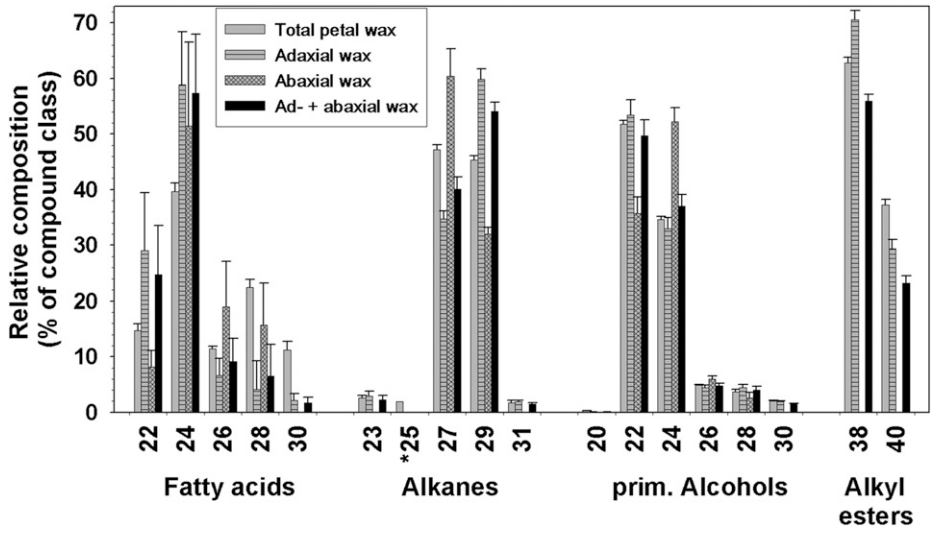

Figure 5. Chain length distributions in cuticular waxes on both sides of the *C. bipinnatus* 'Sensation Pinkie' petal. Relative amounts of each chain length (percentage of compound class) are shown for the wax mixtures extracted from whole petals, adaxial or abaxial side (experimental data; gray bars), or combined adaxial and abaxial wax compositions (calculated data; black bars). The latter were calculated as weighted averages of the adaxial and abaxial waxes to represent the total petal composition determined in two separate steps, for comparison with the experimental values determined directly (plain gray bars; average ± SD; $n = 6$ for total and abaxial waxes, $n = 5$ for adaxial wax). *, C_{25} alkane quantities were calculated based on relative amounts of alkane homologs determined separately after TLC.

of epicuticular and intracuticular waxes taken together closely matched that of the total wax extracted from the abaxial petal side (Fig. 6). Due to low concentrations, some compounds could not be detected or quantified in either the epicuticular or the intracuticular wax sample. Consequently, the chain length distribution of intracuticular fatty acids could not be determined. The overall homolog distributions within all other very-long-chain compound classes of both wax layers appeared very similar (Fig. 7).

Leaf and Stem Waxes

To determine whether petal wax composition is distinct to this organ, leaf and stem waxes were also investigated. Leaves were coated with 12.4 ± 0.8 $\mu g\ cm^{-2}$ wax (Fig. 8), four times the quantity found on petals. Alkanes and primary alcohols dominated, with 4 ± 0.6 and 2.4 ± 0.4 $\mu g\ cm^{-2}$, respectively. Acids (0.5 ± 0.1 $\mu g\ cm^{-2}$), esters (0.2 ± 0.1 $\mu g\ cm^{-2}$), triterpenoid alcohols (1.6 ± 0.3 $\mu g\ cm^{-2}$), and triterpenoid esters (1.8 ± 0.2 $\mu g\ cm^{-2}$) each added less than 15% to the overall wax load. The remainder of the wax (1.6 ± 0.4 $\mu g\ cm^{-2}$) could not be identified. The chain length distributions were similar between the compound classes (Fig. 9), unlike in petals. The longest chain length in the alkanes, alcohols, and free acids was C_{32}, while the shortest chains had 27, 22, and 20 carbons, respectively. The alkane profile was dominated by the C_{29} and C_{31} homologs (40% each), whereas the alcohols and free fatty acids were dominated by C_{28} (50% and 35% respectively) and C_{30} (20% for both). The esters were 46 and 48 carbons in length, with C_{26} and C_{28} alcohols esterified with C_{16}, C_{18}, or C_{20} acids. The triterpenoid alcohols β-amyrin, α-amyrin, and lupeol accumulated in a 1:5:3 ratio in *C. bipinnatus* leaf wax.

The stem wax load (9 ± 2 $\mu g\ cm^{-2}$) was three times that of petal wax. Similar to leaves, alkanes were the most

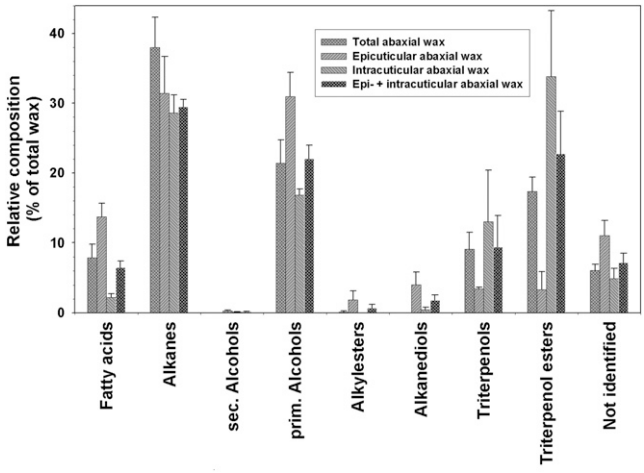

Figure 6. Relative composition of epicuticular and intracuticular waxes on the abaxial side of the *C. bipinnatus* 'Sonata' petal. Relative amounts of compound classes (percentage of total wax) are shown for the total abaxial wax mixture obtained by direct extraction with chloroform, the epicuticular wax sampled with adhesive, and the intracuticular wax extracted afterward (experimental data; gray bars) or combined epicuticular and intracuticular wax compositions (calculated data; black bars). The latter were calculated as weighted averages of the epicuticular and intracuticular waxes to represent the total abaxial wax composition determined in two separate steps, for comparison with the experimental values determined directly (cross-hatched gray bars; average ± SD; $n = 5$ for total abaxial wax, $n = 4$ for epicuticular and intracuticular waxes).

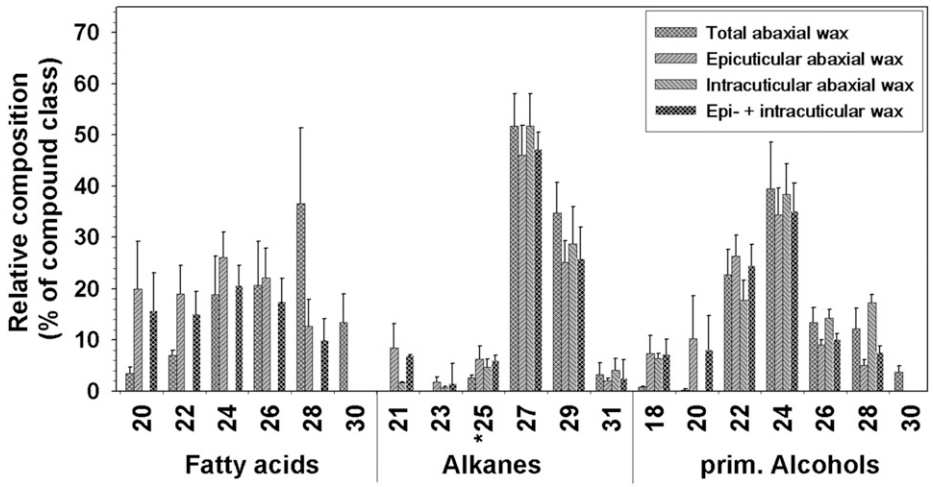

Figure 7. Chain length distributions in epicuticular and intracuticular waxes on the abaxial side of the *C. bipinnatus* 'Sonata' petal. Relative amounts of each chain length (percentage of compound class) are shown for the total abaxial wax mixture obtained by direct extraction with chloroform, the epicuticular wax sampled with adhesive, and the intracuticular wax was extracted afterward (experimental data; gray bars) or combined epicuticular and intracuticular wax compositions (calculated data; black bars). The latter were calculated as weighted averages of the epicuticular and intracuticular waxes to represent the total abaxial wax composition determined in two separate steps, for comparison with the experimental values determined directly (cross-hatched gray bars; average ± SD; $n = 5$ for total abaxial wax, $n = 4$ for epicuticular and intracuticular waxes). *, C_{25} alkane quantities were calculated based on relative amounts of alkane homologs determined separately after TLC.

abundant class (3 ± 2 μg cm^{-2}; Fig. 8). Free fatty acids (1.1 ± 0.3 μg cm^{-2}) and alcohols (0.8 ± 0.3 μg cm^{-2}) made up the rest of the identified straight-chain compounds. Triterpenoid alcohols (0.5 ± 0.3 μg cm^{-2}) and triterpenoid esters (1.0 ± 0.2 μg cm^{-2}) were also present. One-third (2.8 ± 0.7 μg cm^{-2}) of the stem wax mixture remained unidentified. The relative chain length distributions within stem compound classes closely mirrored the distributions found in leaf wax (Fig. 9). Stem wax contained β-amyrin and α-amyrin in a 1:3 ratio but no lupeol.

DISCUSSION

Petal surfaces are the stage for flower-pollinator interactions and thus are expected to be optimized for such a function to the possible detriment of water barrier qualities. Consequently, *C. bipinnatus* wax composition was analyzed and compared with those of the leaves and stems. Major differences between waxes on petals and other organs were found at all three levels: for total wax load, relative quantities of compound classes, and chain length distributions within classes.

First, petals contained only one-quarter to one-third the wax load found on leaves and stems. However, the petal wax load falls within the range of wax loads reported for other organs and species (e.g. approximately 1 and 10 μg cm^{-2} for Arabidopsis leaves and stems, respectively; Jenks et al., 1995). Second, most of the petal wax was primary alcohols, whereas leaf and stem waxes were dominated by alkanes. Primary alcohols may thus play a role in achieving petal-specific functions. Third, the *C. bipinnatus* petal waxes had high concentrations of compounds with chain lengths of C_{20} to C_{24}, in contrast to the C_{28} and C_{30} homologs dominating in the corresponding leaf and stem waxes. The latter chain lengths fall within the typical C_{26} to

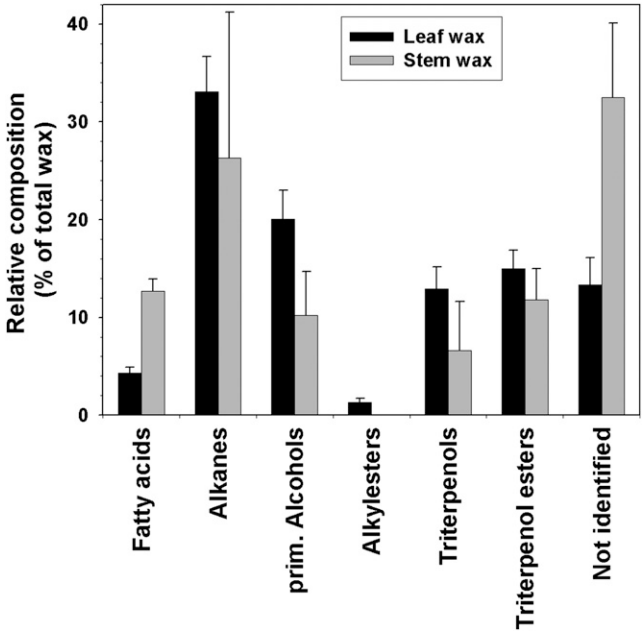

Figure 8. Relative compositions of waxes on the leaves and stems of *C. bipinnatus* 'Sensation Pinkie.' Relative amounts of compound classes (percentage of total wax) are shown (average ± SD; $n = 6$).

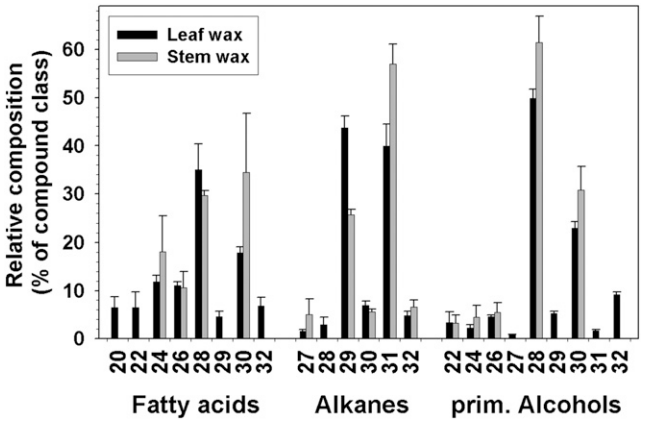

Figure 9. Chain length distribution in waxes on the leaves and stems of *C. bipinnatus* 'Sensation Pinkie.' Relative amounts of each chain length (percentage of compound class) are shown (average ± SD; $n = 6$).

C_{34} range of waxes on vegetative organs (Jetter et al., 2007), whereas the petal wax chain lengths are reminiscent of those in flower waxes from diverse other species (Hennig et al., 1988; Griffiths et al., 2000; Goodwin et al., 2003, King et al., 2007).

Direct comparisons between wax profiles from flower and vegetative organ surfaces had previously been reported only for a few species, in most cases involving shorter chain lengths in flower waxes. Specifically, *P. hybrida* flowers and leaves had C_{22} to C_{28} and C_{28} to C_{32} ester alcohols, respectively (King et al., 2007), and *C. albidus* petals and leaves had mainly C_{38} to C_{40} and C_{42} to C_{46} esters, respectively (Hennig et al., 1988). *V. faba* flower wax was characterized by high levels of C_{22} alcohol (Griffiths et al., 1999), in contrast to either C_{26} or C_{30} alcohols in leaf waxes of the closely related Fabaceae spp. *Phaseolus vulgaris* (Steinmüller and Tevini, 1985), *Medicago truncatula* (Zhang et al., 2005), and *Pisum sativum* (Gniwotta et al., 2005; the composition of *V. faba* leaf wax has not been reported yet). Arabidopsis flower wax is dominated by C_{29} alkane (Shi et al., 2011), shorter than the prevalent C_{31} homolog in leaves (Jenks et al., 1995) but similar to inflorescence stems and siliques (Todd et al., 1999). Overall, there appears to be a fairly widespread compositional pattern in flower waxes, in many species characterized by the presence of shorter chain lengths than on vegetative organs.

Interestingly, the wax on immature leaves of *Prunus laurocerasus* was also dominated by C_{24} fatty acid, alcohol, and acetate, similar to *C. bipinnatus* petal waxes, whereas mature *P. laurocerasus* leaves contained mainly the C_{28} to C_{32} acids and alcohols plus C_{29}/C_{31} alkanes typical of leaves in other species (Jetter et al., 2000; Jetter and Schäffer, 2001). This comparison illustrates that, even though mature organs may have very different wax mixtures, they may still go through developmental stages with very similar compositions. Accordingly, the wax biosynthetic machinery should be relatively similar between different organs at certain ontogenetic stages but may then be reprogrammed during the course of organ development. It will be interesting to test this hypothesis using molecular genetic tools, building on our recently much improved understanding of wax formation in Arabidopsis (Samuels et al., 2008), and broadening it toward homologous enzymes with chain length specificities beyond those of this model species.

Wax composition controls the cuticular functions, of which blocking excessive water loss is typically considered foremost (Kerstiens, 1996; Riederer and Schreiber, 2001). Studies using the same methods as those employed here showed mean water resistances across species for leaves and fruit of 35×10^4 and 1×10^4 s m^{-1}, respectively (Kerstiens, 1996; Schreiber and Riederer, 1996). In comparison, the effectiveness of a petal cuticle at blocking water transport, analyzed, to our knowledge, for the first time in this study, is similar to fruit but only one-tenth of that of typical leaves, thus indicating that *C. bipinnatus* petal cuticles form relatively poor water barriers. This central result of this study can be compared in the future against additional investigations of other species to explore variability between petal waxes and to further test the models explaining cuticular transpiration barriers.

It has been proposed that wax molecules align in parallel in all-trans conformation to form crystalline domains (Small, 1984), which in turn hinder water penetration by forcing individual molecules to weave a tortuous path around them (Reynhardt, 1997; Riederer and Schreiber, 2001). It should be noted that the chain length profiles of different compound classes within *C. bipinnatus* petal waxes differed drastically, with relatively short chain lengths (mainly C_{22}/C_{24}) for fatty acids and primary alcohols and much longer chain lengths (mainly C_{27}/C_{29}) for the co-occurring alkanes. Such a wide chain length distribution of wax constituents is expected to result in a larger volume for water transit surrounding the crystalline domains. Accordingly, wax mixtures constituting both the typical C_{26} to C_{34} compounds and shorter chains should have relatively high permeability. Our overall results on *C. bipinnatus* petal waxes confirm this prediction, as they contained a particularly wide range of chain lengths, including high amounts of C_{20} to C_{24} compounds, and had relatively high permeances.

On the other hand, the effect of relatively short-chain compounds on barrier properties may be challenged by comparing the various *C. bipinnatus* tissues characterized in this study. In a first such comparison, leaf wax had substantially lower amounts of C_{20} to C_{24} alcohols and a much higher permeance than petal wax. However, it must be noted that the *C. bipinnatus* leaf resistance was also lower than the corresponding values reported for most other species to date and, therefore, must be regarded as exceptional. In this context, it should further be noted that both the total wax coverage (μg cm^{-2}) and the water permeances/resistances reported here rely on leaf surface area values that must be taken as rough estimates at best, due to the highly dissected geometry of *C. bipinnatus* leaves. Therefore, *C. bipinnatus* leaf wax may not serve as a good reference for comparing wax

composition and properties. In a second comparison, the adaxial *C. bipinnatus* petal wax contained more C_{20} to C_{24} alcohols and was a more efficient barrier than the abaxial wax, at first sight again suggesting that the shorter chains enhance the transpiration barrier. However, two other factors may also significantly influence the permeability. First, the abaxial wax contains a higher percentage of triterpenoids. As these cyclic compounds likely hamper the formation of crystalline domains, they may consequently increase the permeability of the abaxial surface (Reynhardt, 1997; Riederer and Schreiber, 2001). In addition, the adaxial surface is highly undulated due to the conical cell shapes, which in turn may enhance the effect of the unstirred boundary layer over the surface and add substantially to the water resistance.

In conclusion, our detailed comparisons of wax compositions and physiological properties across various tissues and organs help delineate the various factors influencing overall cuticular barrier properties. As one important result, the water barrier properties of *C. bipinnatus* petal cuticles are likely determined by both the cell surface structure and the particular wax composition, most importantly the chain length distribution of aliphatic wax constituents and the presence and arrangement of cyclic triterpenoids. We hypothesize that C_{20} to C_{24} alcohols decrease the effectiveness of the transpiration barrier while being beneficial for plant-pollinator interactions. To test the effect of small sets of compounds, such as these shorter alcohols, on the structure and properties of a complex wax mixture, it is necessary to study their influence in artificial test systems. For example, appropriate Arabidopsis mutant lines with leaf waxes containing high levels of relatively short alcohols could serve to test their effect on cuticular transpiration.

MATERIALS AND METHODS

Plant Material

Seeds of *Cosmos bipinnatus* 'Sensation Pinkie' (Stokes Seeds) were placed on a nutrient-fortified agar medium (Somerville and Ogren, 1982), stratified for 2 to 3 d at 4°C, and then germinated under continuous light (approximately 150 μmol m^{-2} s^{-1} photosynthetically active radiation) for 1 week at 20°C. Seedlings were transplanted into soil (Sunshine mix 4) and grown under 12-h days/12-h nights at the same intensity as during germination and at 20°C. In addition to frequent watering to keep the soil moist, the plants were watered weekly with MiracleGro. Ray flower petals were harvested 3 to 7 DPA for wax and water permeability analyses for the total petal and adaxial and abaxial surfaces. The distal 3 to 5 cm of leaves originating from nodes 4 to 5 were harvested approximately 2 months after germination and used for wax analyses. For the analyses of the abaxial epicuticular and intracuticular waxes (and entire abaxial wax for comparison) as well as leaves, *C. bipinnatus* 'Sonata' was grown in greenhouses under 14-h days/10-h nights at 22°C/18°C, respectively.

Ray petals were examined by cryoscanning electron microscopy. Samples for measurement were selected to avoid petal margins and vasculature, although these areas were examined to ensure that papillose cells extended over the majority of the petal surface. Specimens were infused with osmium vapor and then plunge frozen in liquid nitrogen. From then on, samples were maintained under vacuum and/or at approximately −150°C. After transfer into a preparatory chamber (Leica EM CPC), surface ice crystals were sublimated at −50°C for 30 min and a probe was used to break the frozen petal to view epidermal cells in cross section. After coating with approximately 8 nm of gold, petal imaging was performed using a Hitachi S4700 field emission scanning electron microscope equipped with a temperature-controlled stage (Emitech K1250 Cryo-System). Alternatively, gold-coated samples were examined using a Hitachi S-2600N variable pressure scanning electron microscope.

ImageJ (Abramoff et al., 2004) was used to measure radii (r) and heights (h) of adaxial epidermis cells from digital images of the samples. From these, the surface area of the conical epidermis cells was calculated assuming paraboloid geometry: $A_{\text{paraboloid}} = (\pi r/6h^2)[(r^2 + 4h^2)^{2/3} - r^3]$. By dividing $A_{\text{paraboloid}}$ by the area of a circle with the same radius ($A_{\text{circle}} = \pi r^2$), a correction factor for the increase in surface area through microscopic relief was calculated. Finally, the effective petal surface area was calculated by multiplying the macroscopic surface area with this correction factor. The resulting microscopic surface areas were used to calculate all wax loads (μg cm^{-2}), water fluxes (kg m^{-2} s^{-1}), and permeances (m s^{-1}) of the adaxial side of the petal. Corresponding values for the overall petal were calculated as weighted averages using macroscopic surface areas for the abaxial side and (corrected) microscopic surface areas for the adaxial side.

Water Permeability Analyses

Water loss was measured following Knoche et al. (2001). Briefly, petals were sealed across the opening of cylindrical water-filled chambers with silicon grease applied along the ring of petal-chamber contact. The surfaces facing the water were scratched to ensure continuous access of water into the petals and thus maintain (as close as possible) 100% internal water concentrations. Chambers were inverted over silica desiccant in order to reduce the external water concentration to essentially 0%, thereby creating a water gradient from 100% to 0% across the cuticle. Samples were equilibrated overnight at 25°C and then inspected for macroscopic failures. Specimens found to have mechanical damage causing bulk water loss were discarded. For all other samples, water loss was measured gravimetrically over up to 12 h. Only water flux values from samples with best-fit linear regression lines of $r^2 > 0.97$ were included for further calculations. Dividing the water flux by the change in water vapor concentration at 25°C yielded the permeance. Permeances are reported as geometric means in accordance with Baur (1997).

For drying experiments, whole organs were harvested, cut surfaces were sealed with liquid paraffin wax (melting point of 46°C–48°C; Merck), and petals were mounted together with silica drying agent inside sealed polypropylene chambers covering a digital balance. Weight loss was recorded every 2.5 min for 1 h, starting after 20 min of equilibration.

Wax Composition Analyses

Waxes were extracted, derivatized, and analyzed as described previously (Greer et al., 2007; Buschhaus and Jetter, 2012). The quantity (μg) was established by comparing peak areas with that of the internal standard. To determine the extracted surface area, apparent surface areas were calculated with ImageJ (Abramoff et al., 2004) software from digital photographs of the samples and multiplied by 2 for total apparent leaf surface area or multiplied by π for total stem surface area. Apparent surface area was used for the flat abaxial petal surfaces, while the apparent surface area was multiplied by 3.8 to obtain the true surface area of the papillose adaxial surface. Wax loads (μg cm^{-2}) were determined by dividing the compound quantity by the corresponding extracted surface area. C_{25} alkane could not be quantified directly within the wax mixture, as it coeluted with a contaminant under our GC conditions. Instead, it was quantified based on relative amounts of alkane homologs within a TLC fraction. All reported wax compound quantities represent averages derived from separate extractions.

Received August 25, 2014; accepted November 17, 2014; published November 20, 2014.

LITERATURE CITED

Abramoff MD, Magelhaes PJ, Ram SJ (2004) Image processing with ImageJ. Biophotonics International **11:** 36–42

Akihisa T, Inoue Y, Yasukawa K, Kasahara Y, Yamanouchi S, Kumaki K, Tamura T (1998) Widespread occurrence of *syn*-alkane-6,8-diols in the flowers of the Compositae. Phytochemistry **49:** 1637–1640

Baur P (1997) Lognormal distribution of water permeability and organic solute mobility in plant cuticles. Plant Cell Environ **20:** 167–177

Bergougnoux V, Caissard JC, Jullien F, Magnard JL, Scalliet G, Cock JM, Hugueney P, Baudino S (2007) Both the adaxial and abaxial epidermal layers of the rose petal emit volatile scent compounds. Planta **226:** 853–866

Buschhaus C, Jetter R (2011) Composition differences between epicuticular and intracuticular wax substructures: how do plants seal their epidermal surfaces? J Exp Bot **62:** 841–853

Buschhaus C, Jetter R (2012) Composition and physiological function of the wax layers coating Arabidopsis leaves: β-amyrin negatively affects the intracuticular water barrier. Plant Physiol **160:** 1120–1129

Buschhaus C, Peng C, Jetter R (2013) Very-long-chain 1,2- and 1,3-bifunctional compounds from the cuticular wax of *Cosmos bipinnatus* petals. Phytochemistry **91:** 249–256

Gniwotta F, Vogg G, Gartmann V, Carver TLW, Riederer M, Jetter R (2005) What do microbes encounter at the plant surface? Chemical composition of pea leaf cuticular waxes. Plant Physiol **139:** 519–530

Goodwin SM, Kolosova N, Kish CM, Wood KV, Dudareva N, Jenks MA (2003) Cuticle characteristics and volatile emissions of petals in Antirrhinum majus. Physiol Plant **117:** 435–443

Greer S, Wen M, Bird D, Wu X, Samuels L, Kunst L, Jetter R (2007) The cytochrome P450 enzyme CYP96A15 is the midchain alkane hydroxylase responsible for formation of secondary alcohols and ketones in stem cuticular wax of Arabidopsis. Plant Physiol **145:** 653–667

Griffiths DW, Robertson GW, Shepherd T, Birch ANE, Gordon SC, Woodford JA (2000) A comparison of the composition of epicuticular wax from red raspberry (*Rubus idaeus* L.) and hawthorn (*Crataegus monogyna* Jacq.) flowers. Phytochemistry **55:** 111–116

Griffiths DW, Robertson GW, Shepherd T, Ramsay G (1999) Epicuticular waxes and volatiles from faba bean (*Vicia faba*) flowers. Phytochemistry **52:** 607–612

Hennig S, Gülz PG, Hangst K (1988) Organ specific composition of epicuticular waxes of *Cistus albidus* L. Cistaceae. Z Naturforsch C **43:** 806–812

Jenks MA, Tuttle HA, Eigenbrode SD, Feldmann KA (1995) Leaf epicuticular waxes of the *eceriferum* mutants in Arabidopsis. Plant Physiol **108:** 369–377

Jenks MA, Tuttle HA, Feldmann KA (1996) Changes in epicuticular waxes on wildtype and *eceriferum* mutants in *Arabidopsis* during development. Phytochemistry **42:** 29–34

Jetter R, Kunst L, Samuels AL (2007) Composition of plant cuticular waxes. *In* M Riederer, C Müller, eds, Annual Plant Reviews 23. Blackwell, Oxford, pp 145–181

Jetter R, Schäffer S (2001) Chemical composition of the *Prunus laurocerasus* leaf surface: dynamic changes of the epicuticular wax film during leaf development. Plant Physiol **126:** 1725–1737

Jetter R, Schäffer S, Riederer M (2000) Leaf cuticular waxes are arranged in chemically and mechanically distinct layers: evidence from *Prunus laurocerasus* L. Plant Cell Environ **23:** 619–628

Kerstiens G (1996) Cuticular water permeability and its physiological significance. J Exp Bot **47:** 1813–1832

King A, Nam JW, Han J, Hilliard J, Jaworski JG (2007) Cuticular wax biosynthesis in petunia petals: cloning and characterization of an alcohol-acyltransferase that synthesizes wax-esters. Planta **226:** 381–394

Knoche M, Peschel S, Hinz M, Bukovac MJ (2001) Studies on water transport through the sweet cherry fruit surface. II. Conductance of the cuticle in relation to fruit development. Planta **213:** 927–936

Reynhardt EC (1997) The role of hydrogen bonding in the cuticular wax of *Hordeum vulgare* L. Eur Biophys J **26:** 195–201

Riederer M, Schreiber L (1995) Waxes: the transport barriers of plant cuticles. *In* **RJ Hamilton**, ed, Waxes: Chemistry, Molecular Biology and Functions. Oily Press, West Ferry, UK, pp 131–156

Riederer M, Schreiber L (2001) Protecting against water loss: analysis of the barrier properties of plant cuticles. J Exp Bot **52:** 2023–2032

Salasoo I (1989) Epicuticular wax hydrocarbons of Ericaceae in British Columbia. Biochem Syst Ecol **17:** 381–384

Samuels L, Kunst L, Jetter R (2008) Sealing plant surfaces: cuticular wax formation by epidermal cells. Annu Rev Plant Biol **59:** 683–707

Schönherr J (1976) Water permeability of isolated cuticular membranes: the effect of cuticular waxes on diffusion of water. Planta **131:** 159–164

Schreiber L, Riederer M (1996) Ecophysiology of cuticular transpiration: comparative investigation of cuticular water permeability of plant species from different habitats. Oecologia **107:** 426–432

Shi JX, Malitsky S, De Oliveira S, Branigan C, Franke RB, Schreiber L, Aharoni A (2011) SHINE transcription factors act redundantly to pattern the archetypal surface of Arabidopsis flower organs. PLoS Genet **7:** e1001388

Small DM (1984) Lateral chain packing in lipids and membranes. J Lipid Res **25:** 1490–1500

Somerville C, Ogren W (1982) Isolation of photorespiratory mutants of Arabidopsis. *In* R Hallick, N Chua, eds, Methods in Chloroplast Molecular Biology. Elsevier, New York, pp 129–139

Steinmüller D, Tevini M (1985) Action of ultraviolet radiation (UV-B) upon cuticular waxes in some crop plants. Planta **164:** 557–564

Stoianova-Ivanova B, Mladenova K, Popow S (1971) The composition and structure of ketones from rose bud and rose flower waxes. Phytochemistry **10:** 1391–1393

Todd J, Post-Beittenmiller D, Jaworski JG (1999) *KCS1* encodes a fatty acid elongase 3-ketoacyl-CoA synthase affecting wax biosynthesis in *Arabidopsis thaliana*. Plant J **17:** 119–130

Whitney HM, Bennett KMV, Dorling M, Sandbach L, Prince D, Chittka L, Glover BJ (2011) Why do so many petals have conical epidermal cells? Ann Bot (Lond) **108:** 609–616

Wollrab V (1969a) On natural waxes. XIII. Composition of the oxygenous fractions of rose blossom wax. Collect Czech Chem Commun **34:** 867–874

Wollrab V (1969b) Secondary alcohols and paraffins in the plant waxes of the family Rosaceae. Phytochemistry **8:** 623–627

Zhang JY, Broeckling CD, Blancaflor EB, Sledge MK, Sumner LW, Wang ZY (2005) Overexpression of WXP1, a putative Medicago truncatula AP2 domain-containing transcription factor gene, increases cuticular wax accumulation and enhances drought tolerance in transgenic alfalfa (Medicago sativa). Plant J **42:** 689–707